

## *ESO observing programme GCAV: Galaxy Clusters At Vircam (198.A-2008 PI. M. Nonino)*

### Abstract

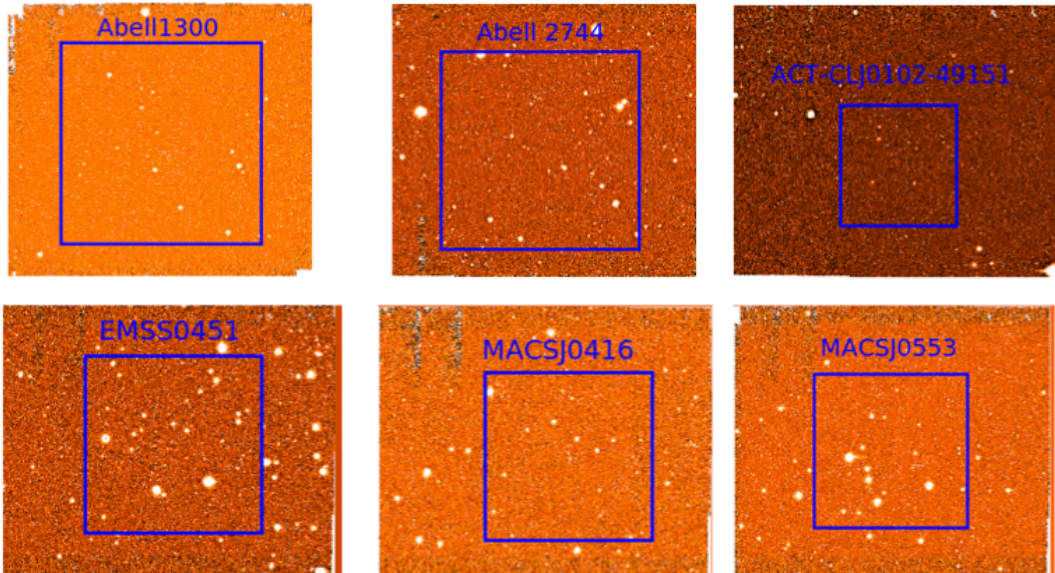
We release coadded tiles and related source lists, at tile level, from data collected for the ESO Programme 198.A-2008 from Oct 2016 to the end of Feb 2020 with VISTA/VIRCAM in Y,J,Ks bands. The GCAV Programme aims at observing 20 massive galaxy clusters which have also been observed in many ground based and spaced based programs (e.g. CLASH, RELICS, HFF/BUFFALO). This release concerns 15 clusters. This is the second release (DR2) of data for the 198.A-2008 Programme and contains 308 OBs collected in P98 to P104, with ESO grade A and B. The area covered by the observations sum to  $\sim 26.28 \text{ deg}^2$  in the three bands ( $\sim 1.75 \text{ deg}^2$  per cluster/filter).

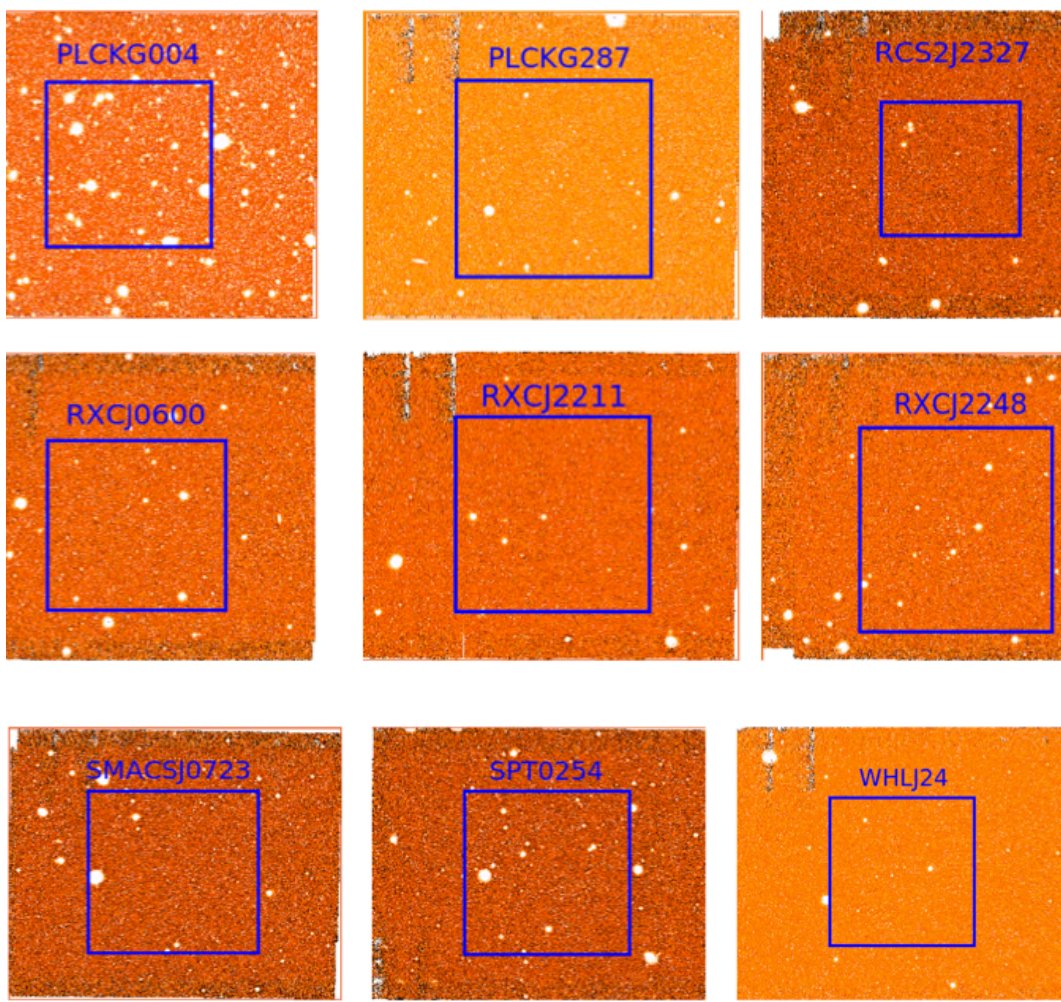
### Overview of Observations

Observations for the ESO Programme 198.A-2008 area carried out in Obs 63.25 min long in Y and J, and 61.25 min long in Ks. The pattern is the Tile6n with on sky exposures of 48 min in Y and J and 42 min in Ks. For each Y and J exposures, DIT is set to 30s., NDIT to 2 and NJITTER to 8; for Ks exposures DIT is 10s., NDIT is 6 and NJITTER is 7.

The 15 clusters included in this release are: **Abell 1300**, **Abell 2744**, **ACT-CLJ0102-49151**, **EMMS0451-0306**, **MACSJ0416.1-2403**, **MACSJ0553.4-3342**, **PLCKG004.5-19.15**, **PLCK-G287+32.9**, **RCS2J2327.6-020437**, **RXCJ0600.1-2007**, **RXCJ2211.7-0350**, **RXCJ2248.7-443143**, **SMACSJ0723.3-7327**, **SPT-CLJ0254-5857**, **WHLJ243324-8.477**.

The following finding charts show the observed fields for each cluster. The box is 15 Mpc physical size at cluster redshift (Planck cosmology, e.g. Aghnim et al. 2018).





#### Release Content

**TABLE 1.** Summary of the released images and source lists per cluster at OB level:

Cluster FieldID	RJ2000 DECJ2000	Filt er	N. OB s	Total exptime (sec.)	Eptime per pix- el (sec.)	Psf FWHM,mi n:max, arcsec	MagLim(AB ,min:max	Size im- ages+we ights+so urce lists (Gb)
Abell 1300	11:32:20.0 -19:45:00.0	Y	8	23040	7680	0.73:1.13	23.24:23.65	32.78
		J	7	20100	6700	0.75:1.22	23.20:23.76	29.45
		Ks	5	12600	4200	0.62:0.89	22.34:22.60	20.24
Abell 2744	00:14:15.0 -30:35:30.0	Y	6	17280	5760	0.67:1.11	23.29:23.88	25.62

		J	2	5760	1920	0.68:0.69	23.58:23.75	8.43
		Ks	4	9720	3240	0.82:1.09	22.36:22.52	17.09
ACT-CLJ 0102-491 51	01:04:30.0 -49:09:30.0	Y	8	22080	7360	0.69:0.96	23.43:23.74	33.46
		J	6	17100	5700	0.91:1.14	23.09:23.90	25.09
		Ks	2	5040	1680	0.73:0.97	22.82:22.84	8.22
EMM- S0451-03 06	04:54:17.0 -03:00:15.0	Y	10	28620	9540	0.77:1.23	23:30:23.86	41.99
		J	8	23280	7760	0.75:0.97	23.28:23.66	33.30
		Ks	9	21720	7240	0.77:0.97	22.32:22.73	37.93
MACSJ 0416.1-24 03	04:16:30.0 -24:02:30.0	Y	10	28800	9600	0.77:0.97	23.29:23.56	42.18
		J	6	17280	5760	0.71:0.92	23.06:23.53	25.36
		Ks	8	20160	6720	0.70:1.13	22.33:22.46	33.70
MACSJ 0553.4-33 42	05:53:55.0 -33:35:00.0	Y	8	22500	7500	0.71:1.16	23.09:23.78	33.07
		J	7	20160	6720	0.65:0.86	23.23:23.74	29.32
		Ks	5	12060	4020	0.73:0.83	22.28:22.53	20.68
PLCK- G004.5-19 .15	19:18:00.0 -33:25:30.0	Y	12	34560	11520	0.74:1.20	23.18:23.80	51.19
		J	12	34560	11520	0.73:0.95	23.21:23.64	51.21
		Ks	11	27900	9300	0.67:0.82	22.37:22.53	46.68
PLCK- G287+32. 9	11:51:00.0 -28:10:00.0	Y	5	14520	4840	0.75:0.83	23.33:23.66	20.95
		J	3	8640	2880	0.74:0.76	23.44:23.54	12.58
		Ks	3	7560	2520	0.74:0.92	22.12:22.34	12.67
RCS2J 2327.6-02 0437	23:27:00.0 -02:02:15.0	Y	13	37440	12480	0.66:1.29	23.07:23.65	54.30
		J	11	31680	10560	0.73:1.18	23.05:23.67	45.79
		Ks	5	12600	4200	0.67:0.84	22.28:22.47	20.61
RXCJ 0600.1-20 07	06:00:35.0 -19:59:45.0	Y	10	23380	9460	0.72:1.26	23.03:23.65	41.68
		J	7	20100	6700	0.71:1.08	23.22:23.58	29.22

		Ks	7	17640	5880	0.69:0.90	22.33:22.66	29.07
RXCJ 2211.7-03 50	22:12:30.0 -03:45:00.0	Y	10	28800	9600	0.70:0.87	23.24:23.86	41.25
		J	8	23040	7680	0.62:1.04	23.18:23.55	33.10
		Ks	7	17640	5880	0.63:0.90	22.30:22.36	29.11
RXCJ 2248.7-44 3143	22:49:30.0 -44:22:30.0	Y	4	11520	3840	0.67:0.93	23.27:23.88	16.86
		J	1	2880	960	0.84	23.22	4.17
		Ks	5	12600	4200	0.67:0.84	22.31:22.51	20.83
SMACSJ 0723.3-73 27	07:25:00.0 -73:20:00.0	Y	3	8640	2880	0.78:0.91	23.45:23.63	12.48
		J	8	23040	7680	0.73:1.41	22.80:23.64	32.79
		Ks	8	20100	6700	0.83:1.20	21.99:22.36	33.01
SPT-CLJ 0254-585 7	02:55:40.0 -58:50:00.0	Y	6	17280	5760	0.65:1.23	23.34:23.78	24.76
		J	4	11220	3740	0.73:0.77	23.47:23.75	16.34
		Ks	9	22620	7540	0.83:1.16	22.36:22.80	37.21
WHLJ2433 24-8.477	01:37:10.0 -08:20:00.0	Y	8	22980	7660	0.78:1.07	23.51:23.85	33.65
		J	8	22680	7560	0.76:0.97	23.12:24.07	33.59
		Ks	1	2520	840	0.84	22.34	4.16
							Total	1287.17

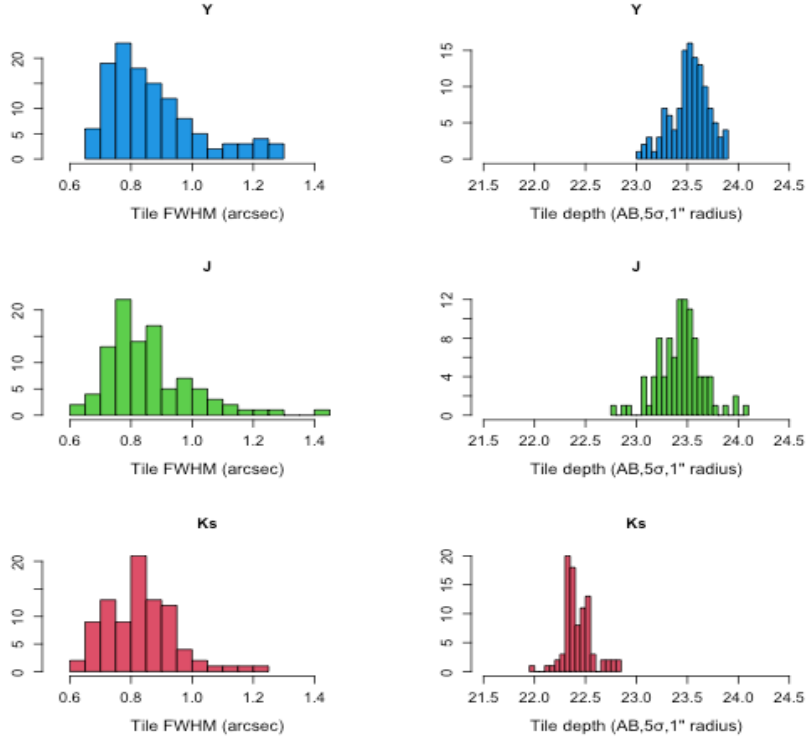
The limiting mag is  $5\sigma$  within 1'' radius aperture and includes aperture correction to 5'' aperture radius:  $\text{MagLim} = \text{ZP} - 2.5 \cdot \log_{10}(5 \cdot \sqrt{\pi \cdot 25} \cdot \text{skyrms}) - \text{APCORR1}$

The plot shows the distribution of the estimated FWHM and  $5\sigma$  depth of the released tiles, in Y,J and Ks.

## Release Notes

### Data Reduction and Calibration

- Data reduction has been performed with a pipeline written in Julia ([www.julialang.org](http://www.julialang.org)) which develops e.g. Nonino et al. 2009, and performs the following steps:
- Linearity correction following <http://casu.ast.cam.ac.uk/surveys-projects/vista/technical/data-processing/design.pdf/view>
- Dark correction, subtracting the associated dark image, created from median combination of nightly darks, and matching the DIT value of the given science exposures.



- De-stripping, which removes the low-level horizontal striping due to VIRCAM detector readout electronic.
- Flat field correction, dividing by a median of twilight sky images also compensating for different gain in the different detectors.
- Creation of statics masks which flag pixels with substantial deviates in the dark and flat calibration images. These pixels are assigned weight 0.
- Astrometric solution is performed against GAIA DR2 sources (<https://gea.esac.esa.int/archive>), using Scamp (v2.0.4, Bertin 2006). The systematics in the coadded images are at the level of 10 mas and less, and rms  $\sim 20$  mas with respect to GAIA sources. The density of used GAIA sources per VIRCAM ranges from  $\sim 100$  to 500 depending upon the cluster.
- Photometry: the zero point of each coadded tile has been derived from comparison of aperture corrected magnitudes of bright but unsaturated sources with the aperture corrected magnitude from the source lists delivered by the VISTA Data Flow System (Irwin et al. 2004, Hambly et al. 2008, Cross et al., 2012). This has also been used to apply a final illumination correction (at the level of the stack). For a very detailed analysis of the VISTA photometric system, including Vega to AB conversion, we refer to Gonzales-Fernandez et al. (2018, MNRAS, 474). The comparison of bright unsaturated sources results in a median and mean rms of 0.037 indicative of the limits of photometric systematics of the released data. Further comparisons of aperture corrected magnitudes against VIKING, VHS observations partly overlapping released clusters confirm this result. Further check on the photometric calibration has been performed stacking chip by chip each OB. This resulted in 96 stacks for each OB, for which PSF has been estimated, using PSFex (v3.21.1, Bertin, 2011): photometry of bright, not saturated stars has been compared with 2MASS sources, confirming the obtained zero points (RMS  $< 0.05$ ) in the AB interval  $\sim 13.5$ -15.5.
- Background subtraction: this step is performed using the astrometric solutions to mask each pixel, in the dark and flat corrected images, which in the coadded stack has been mapped into a detected object. Defect such as satellite tracks have been masked with the mask incorporated in the single image weight map.
- Tile and deep stacks are obtained using a slightly modified version of Swarp (v2.19.1, Bertin et al. 2002).
- Psf obtained via PSFex (v3.2.11, Bertin, 2011).

Released source lists have been obtained using SExtractor (v2.19.5, Bertin & Arnouts 1996). Purity has been preferred to completeness, in order to minimize spurious detections. Running Sex-

tractor on the inverted images (additive inverse) result in a fraction of  $< .001$  of spurious sources, due to noise in the image background, see also Known Issues below, for the selected parameters.

Relevant parameters:

```
DETECT_MINAREA 9
DETECT_THRESH 4
THRESH_TYPE RELATIVE
FILTER Y
FILTER_NAME gauss_1.5_3x3.conv
DEBLEND_NTHRESH 32
DEBLEND_MINCONT 0.00005
CLEAN Y
CLEAN_PARAM 1
MASK_TYPE CORRECT
PHOT_AUTOPARAMS 2.5,3.5
BACK_SIZE 256
BACK_FILTERSIZE 2
BACKPHOTO_TYPE LOCAL
BACKPHOTO_THICK 24
```

## Data Quality

- The astrometry has been performed using GAIA2 as reference: systematics and random errors are listed in the header of the images CSYER1, CSYER2, CRDER1, CRDER2 (units degrees).
- Adopted conversions to AB (Gonzales-Fernandez et al. 2018, D3, D4 and D6):  
Y\_AB(+0.600), J\_AB(+0.916), Ks\_AB(+1.827)
- Magnitudes from aperture radii of 1", 1".5, 2", 2".5, 3", 4" and PSFMag have been corrected to aperture radius 5", for each stacked tile. Magnitudes have **NOT** been corrected for Galactic extinction.
- The uniformity of the MagLim, which has been obtained placing 10000 apertures over the whole images, but retaining only those not contaminated by sources, as from the segmentation map, and with all pixels having weight  $\neq 0$  is exemplified in the following figure
- The zeropoints are uniform across each tile.

## Known issues

Varying quantum efficiency in detector 16 result in problematic regions in the coadded images as can be seen in the 5 sigma depth figure (top left region). In the current release, the most common source of spurious objects in source lists is associated with diffraction halos and filter-reflection ghosts around bright stars; these are easily recognized in the parent images since they are mostly localized around bright stars.

## Previous Releases

This Release follows DR1, adding new OBs.

## Data Format

### Files Types

The naming convention for the released data is

science image

gcav\_\$CLUSTER\_NAME\$\_\$FILTER\$\_\$OBID\$\_\$CREATION\_DATE\$\_g2sw.fits

associated weight image

gcav\_\$CLUSTER\_NAME\$\_\$FILTER\$\_\$OBID\$\_\$CREATION\_DATE\$\_g2sw.weight.fits

associated source source list

gcav\_\$CLUSTER\_NAME\$\_\$FILTER\$\_\$OBID\$\_\$CREATION\_DATE\$\_g2sw\_cat.fits

### Catalogue Columns

No	Column Name	Column Description
1	SOURCENAME	IAU-formatted name, prefixed with "GCAV"
2	SOURCEID	Running object number
3	RA2000	Right ascension of barycenter (J2000)
4	DEC2000	Declination of barycenter (J2000)
5	MAG_AUTO	Kron-like elliptical aperture magnitude
6	MAGERR_AUTO	RMS error for Kron-like elliptical aperture magnitude
7	KRON_RADIUS	Kron aperture
8	MAG_ISO	Isophotal magnitude
9	MAGERR_ISO	RMS error for isophotal magnitude
10	MAG_APER1	Aperture corrected magnitude within 1" radius
11	MAG_APER2	Aperture corrected magnitude within 1".5 radius
12	MAG_APER3	Aperture corrected magnitude within 2" radius
13	MAG_APER4	Aperture corrected magnitude within 2".5 radius
14	MAG_APER5	Aperture corrected magnitude within 3" radius
15	MAG_APER6	Aperture corrected magnitude within 4" radius
16	MAG_APER7	Aperture magnitude within 5" radius
17	MAG_APER8	Aperture magnitude within 7".5 radius
18	MAG_APER9	Aperture magnitude within 10" radius
19	MAGERR_APER1	RMS error for aperture 1
20	MAGERR_APER2	RMS error for aperture 2
21	MAGERR_APER3	RMS error for aperture 3
22	MAGERR_APER4	RMS error for aperture 4
23	MAGERR_APER5	RMS error for aperture 5
24	MAGERR_APER6	RMS error for aperture 6

25	MAGERR_APER7	RMS error for aperture 7
26	MAGERR_APER8	RMS error for aperture 8
27	MAGERR_APER9	RMS error for aperture 9
28	FRAD90	Fraction-of-light radius at 90%
29	FLAGS	SExtractor flag
30	CLASS_STAR	SExtractor Star/Galaxy classification (0-galaxy,1-star)
31	FWHM_IMAGE	FWHM assuming a gaussian core (pixels)
32	BACKGROUND	Background at centroid position
33	A_IMAGE	Isophotal major axis
34	B_IMAGE	Isophotal minor axis
35	THETA_IMAGE	Isophotal image position angle
36	MAG_PSF	Magnitude from PSF-fitting
37	MAGERR_PSF	RMS error from PSF-fitting
38	MAG_MODEL	Magnitude from model-fitting
39	MAGERR_MODEL	RMS error for model-fitting magnitude
40	SPREAD_MODEL	Spread parameter from model-fitting
41	SPREADERR_MODEL	RMS error for spread parameter from model-fitting
42	MAG_POINTSOURCE	Point source total magnitude from fitting
43	MAGERR_POINTSOURCE	RMS error for fitted point source total magnitude
44	MAG_PETRO	Petrosian-like aperture magnitude
45	MAGERR_PETRO	RMS error for Petrosian-like aperture magnitude
46	PETRO_RADIUS	Petrosian radius

## Acknowledgements

- "Based on data products created from observations collected at the European Organisation for Astronomical Research in the Southern Hemisphere under ESO programme(s) 198.A-2008(A), 198.A-2008(B), 198.A-2008(C), 198.A-2008(D), 198.A-2008(E), 198.A-2008(F), 198.A-2008(G)"
- "This research has made use of the services of the ESO Science Archive Facility."

*Science data products from the ESO archive may be distributed by third parties, and disseminated via other services, according to the terms of the [Creative Commons Attribution 4.0 International license](#). Credit to the ESO origin of the data must be acknowledged, and the file headers preserved.*